

Effects of Intake Components on Combustion and Emission Characteristics in an *n*-Butanol/Diesel Blend Fueled Engine

Wanchen Sun, Xin Zhang, Liang Guo, Yi Sun, Yuying Yan, Jun Li, Hao Zhang,* and Dongqi Fu

Cite This: *ACS Omega* 2021, 6, 16129–16139

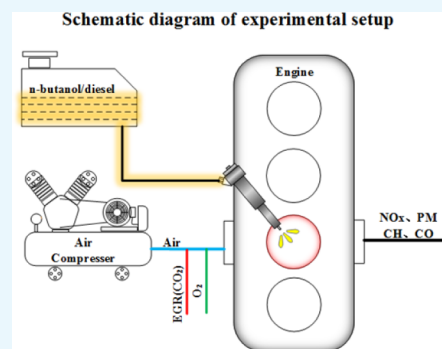
Read Online

ACCESS |

Metrics & More

Article Recommendations

ABSTRACT: To assess the effects of intake components and *n*-butanol application on compression-ignition engines, an experiment was carried out based on a single-cylinder engine fueled with *n*-butanol/diesel-blended fuel. The results show that with the increased *n*-butanol fraction of the blended fuel, the emissions of particulate mass (PM) decrease significantly, but the NO_x and hydrocarbon (HC) emissions deteriorate. For B15 and B30, the PM emissions are 66.2% and 74.4% lower than B0, respectively. Furthermore, exhaust gas recirculation (EGR) was introduced to reduce the NO_x emissions. However, a large EGR rate significantly reduces the indicated thermal efficiency (ITE) of the engine. Compared with the non-EGR condition, the ITE of B15 and B30 decrease by 3.1% and 3.8%, respectively, when the EGR rate is 18%. At the same time, the PM and HC emissions are found to be increased greatly. The PM emission of B15 and B30 increases by 69% and 46% and the HC emission increase by 150% and 71%, respectively. To restrain the engine emissions caused by the EGR, pure oxygen is further introduced into the intake charge. It is found that both the PM and HC emissions are significantly reduced with the introduction of extra oxygen. Under the condition of the 18% EGR rate, increasing oxygen addition to 4% can reduce HC emissions by more than 50% and the total particle mass of B15 and B30 is reduced by 60.6% and 47.7%, respectively. Moreover, the ITE reduction and combustion deterioration caused by the large EGR are found to be alleviated. By adjusting the *n*-butanol ratio, EGR rate, and oxygen addition, the excellent performance of combustion and emission can be achieved in an *n*-butanol/diesel blend fueled engine.



1. INTRODUCTION

The compression-ignition (CI) engines are widely used in transportation and other fields due to their high thermal efficiency, excellent power output, and durability. However, due to the inhomogeneous mixture in the cylinder, various toxicological pollutants are inevitably generated during the combustion process of the diesel engine.^{1–4} As the number of engines keeps growing, environmental problems are becoming more and more severe. Research shows that among the nonroad mobile sources, such as CO, hydrocarbon (HC), NO_x, and particulate mass (PM) emissions, the proportion of diesel engines exhaust exceeds 66%, and countries around the world have also introduced increasingly strict emission regulations to limit diesel engine pollutant emissions.^{5,6} However, with the development of human society, the demand for nonrenewable energy is also growing. Therefore, it is necessary to find alternative renewable resources, improve the thermal efficiency of diesel engines, and reduce pollutant emissions.^{7–11}

In recent years, butanol has been widely studied as a liquid alternative fuel with great development potential.^{12–14} Butanol is an alcohol fuel with four C atoms, and its molecular formula is C₄H₉OH. As a second-generation biofuel, butanol has the advantages such as high energy density, low volatility, low

corrosiveness, and good miscibility with diesel and gasoline, making it a potential alternative fuel.^{15,16} At the same time, with the continuous development of microbial fermentation technology, the manufacturing process of biobutanol based on renewable raw materials has gradually matured. Biobutanol has made great progress in terms of the raw material adaptability and product conversion rate. Therefore, the production cost of butanol has been greatly reduced, and it has a broad market application prospect.^{17,18} At present, extensive research has been conducted on the application of butanol fuel to vehicle internal combustion engines. Among them, blending butanol with diesel and then injecting the blended fuel into the cylinder is the main method of butanol application in the CI engines.^{19–21} Rakopoulos et al.²² experimentally studied the effects of butanol/diesel-blended fuels on the combustion and emissions of CI engines. The results showed that compared

Received: April 15, 2021

Accepted: May 31, 2021

Published: June 8, 2021



with diesel, the soot, NO_x , and CO emissions were reduced in different degree, but the HC emissions increased when using the butanol/diesel-blended fuels. Gu et al.²³ and Yao et al.²⁴ compared the effects of butanol and its isomers on the emission characteristics of a CI engine, and they concluded that the NO_x and soot emissions can be further reduced by the coordination of exhaust gas recirculation (EGR) and injection strategies. However, owing to the higher latent heat of vaporization and the lower cetane number of the blended fuel, the load range of the butanol/diesel engine was narrow. Some results showed that burning *n*-butanol/diesel-blended fuel cause the increase in emissions such as HC and CO, and these problems are more obvious after the introduction of EGR.^{25,26}

To solve the problems of engine burning *n*-butanol/diesel-blended fuel, it is necessary to adopt oxygen-enriched combustion technology. Oxygen-enriched combustion of diesel engines has a positive effect on improving the thermal efficiency and reducing pollutant emissions. Early studies have found that oxygen has a direct and significant effect on the in-cylinder combustion process. Therefore, increasing the oxygen content of the intake gas can improve the combustion efficiency and reduce fuel consumption and pollutant emissions such as HC, PM, and CO.^{27,28} Moreover, the activation atmosphere produced by adding oxygen is conducive to the combustion of the mixed gas, which is beneficial to alleviating the problem of narrow load range when the engine is fueled with the *n*-butanol/diesel-blended fuel. In the early days, due to the limitation of the cost for oxygen-enriched technology, oxygen-enriched combustion was mainly used in the field of thermal power generation. In recent years, profiting from the rapid development of the gas membrane separation technology, it has the basics for the application of oxygen-enriched combustion technology on engines.^{29–32}

A number of studies showed that the combination of *n*-butanol/diesel blends and EGR can reduce the NO_x and soot emissions of the engine, but with an increased EGR rate, the thermal efficiency and HC emission of the engine deteriorate gradually. To restrain the adverse effects of the large EGR rate, oxygen-enriched technology was adopted in the experiment by a modified intake system. The combined effects of the *n*-butanol/diesel-blended fuel and intake components on combustion and emission of the engine were explored in this study.

2. RESULTS AND DISCUSSION

2.1. Effects of Fuel Characteristics on Combustion and Emissions. Figures 1 and 2 show the combustion characteristics of the engine for different fuels. It can be seen from the figures that with the increased *n*-butanol-blended ratio, the maximum cylinder pressure and the rate of heat release (RoHR) are obviously increased, and the reason is that the *n*-butanol addition leads to a larger proportion of premixed combustion. It can also be seen from the figures that with the increased *n*-butanol-blended ratio, the ignition delay (ID) is obviously prolonged and the combustion duration (CD) is shortened. Compared with fuel B0, the ID of fuel B15 and B30 is prolonged by 2.9 and 4.6 deg CA, respectively, and the CD is shortened by 2.8 and 4.9 deg CA, respectively. The lower cetane number and higher latent heat of vaporization of the blended fuel are the two major factors that contribute to a lower cylinder temperature during the fuel atomization stage; hence, the ID is obviously prolonged with the increased *n*-

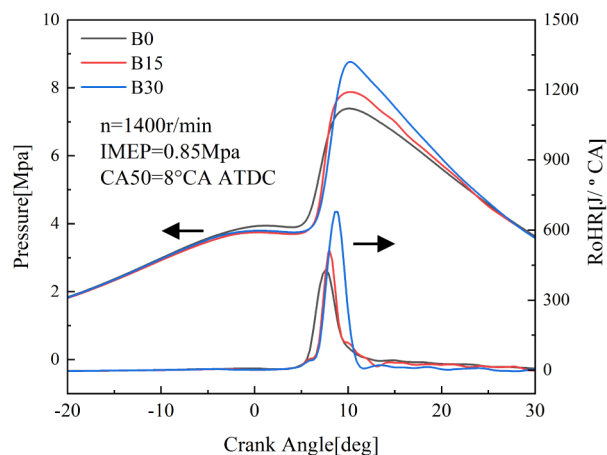


Figure 1. Cylinder pressure and RoHR of different fuels.

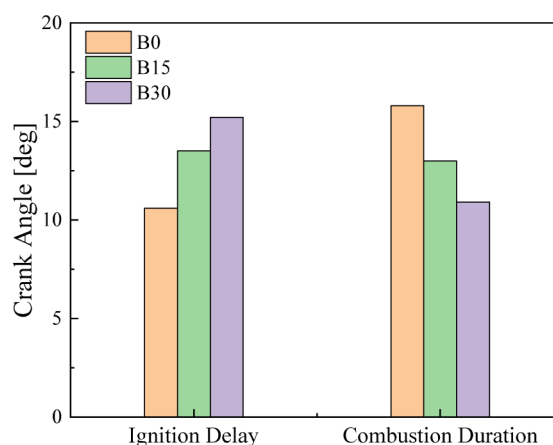


Figure 2. ID and CD of different fuels.

butanol-blended ratio. In addition, the longer ID is conducive to increasing the proportion of premixed combustion and thereby shortening the CD. It can improve the fuel atomization effect and thus reduce the engine pollutant emissions.

Figure 3 shows the NO_x and HC emissions of different fuels. It can be observed that both the NO_x and HC emissions are increased for B15 and B30 compared with the pure diesel. The higher *n*-butanol-blended ratio increases the maximum RoHR, which leads to a higher combustion temperature. The *n*-butanol addition increases the oxygen content in the cylinder, and the effects of combustion temperature and oxygen

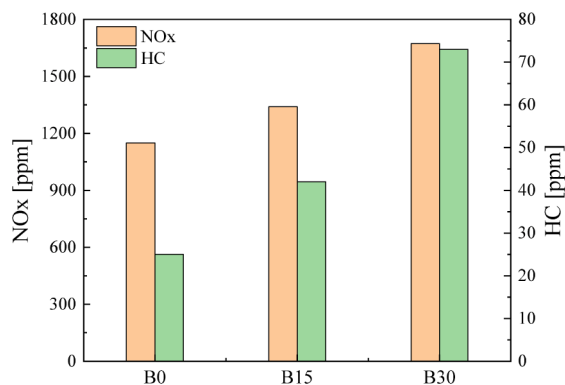


Figure 3. NO_x and HC emissions of different fuels.

concentration promote the production of NO_x . The reason for the increase in HC emissions is that the long ID of the blended fuels leads to a large amount of fuel adhering to the wall of cylinder chamber, and it is difficult to burn completely due to the low temperature and oxygen concentration near the wall. Figure 4 shows the PM emissions of different fuels. In this

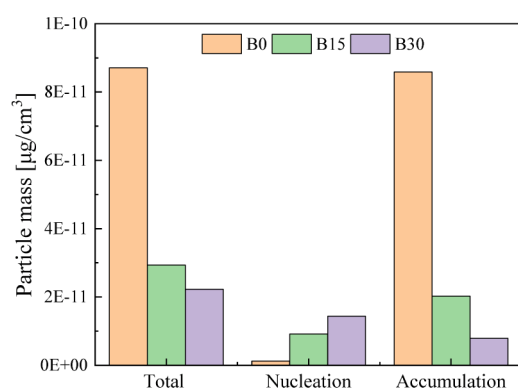


Figure 4. PM emissions of different fuels.

paper, the particle whose size is in 0–35 nm is defined as a nuclear mode particle (NMP), and the particle whose size is larger than 35 nm is defined as the accumulation mode particle (AMP). For B15 and B30, the total PM emissions are 66.2% and 74.4% lower than B0, respectively, but the NMP mass emissions increase with the increased *n*-butanol-blended ratio. It illustrates that the higher oxygen content of *n*-butanol/diesel blends promote the oxidation of AMP. However, the reason why the NMP increases is that the HC emissions of *n*-butanol/diesel blends are higher, and the saturated HC components condense to the NMP during the cooling and dilution processes of the exhaust gas.

In summary, burning *n*-butanol/diesel blends increases the proportion of premixed combustion, improves the volumetricity of combustion, and reduces particulate emissions significantly, but at the same time it increases the NO_x and HC emissions.

2.2. Effects of EGR on Combustion and Emissions of *n*-Butanol/Diesel Blends. To avoid the deterioration of NO_x emissions when burning *n*-butanol/diesel blends, the effects of different EGR rates on the combustion and emissions for *n*-butanol/diesel blends were experimentally studied. B15 and

B30 were selected as the tested fuels for the EGR rates including 0%, 10%, 14%, and 18%.

Figure 5 shows the ID and CD of B15 and B30 at different EGR rates. It can be seen from Figure 5a that the ID for both blended fuels is prolonged with the increased EGR rate. It is because that the introduction of EGR gas increases the specific heat capacity of the working medium in the cylinder, thereby reducing the in-cylinder temperature. Moreover, the introduction of EGR gas also reduces the oxygen concentration in the cylinder. Both the reasons are not conducive to achieving the ignition conditions of the mixture. In addition, due to the lower cetane number and higher latent heat of vaporization, the ID for B30 is about 2–3 deg CA longer than that of the B15 at all EGR rates. Figure 5b shows that the CD of both fuels decreases with an increase in the EGR rate. The main reason for this result is that the increase in the EGR rate prolongs the ID, which leads to an increasing premixed combustion ratio and a higher combustion speed. Furthermore, the low oxygen concentration caused by EGR may lead to incomplete combustion of the fuel at the last stage of the combustion process and shortens the CD. Comparing the CD for two fuels at different EGR rates, it can be found that the CD for B30 is 2–3 deg CA shorter than B15, and because of this more fuel is consumed in the premixed combustion for B30.

Figure 6 shows the thermal efficiency and pollutant emissions of B15 and B30 at different EGR rates. It can be found that the indicated thermal efficiency (ITE) decreases significantly with the increased *n*-butanol-blended ratio and EGR rate. Compared with non-EGR conditions, the ITE of B15 and B30 decreases by 3.1% and 3.8%, respectively, when the EGR rate is 18%. The reason for the decrease in the ITE should be that the lower heat value and the higher latent heat of vaporization of *n*-butanol result in a decrease in the cycle heat release and an increase in the heat absorption. Moreover, the decrease in the ITE caused by EGR could be explained by the fact that EGR can reduce the oxygen content in the cylinder, and the specific heat capacity of triatomic molecular gases in EGR is larger than diatomic molecular gases (air), which leads to a decrease in combustion temperature and combustion efficiency. In addition, the effects of EGR are beneficial to suppressing the generation of NO_x but not conducive to improving the particulate and HC emissions. At an EGR rate of 18%, the NO_x emission of B15 and B30 decreases by 55% and 53%, the total particle mass

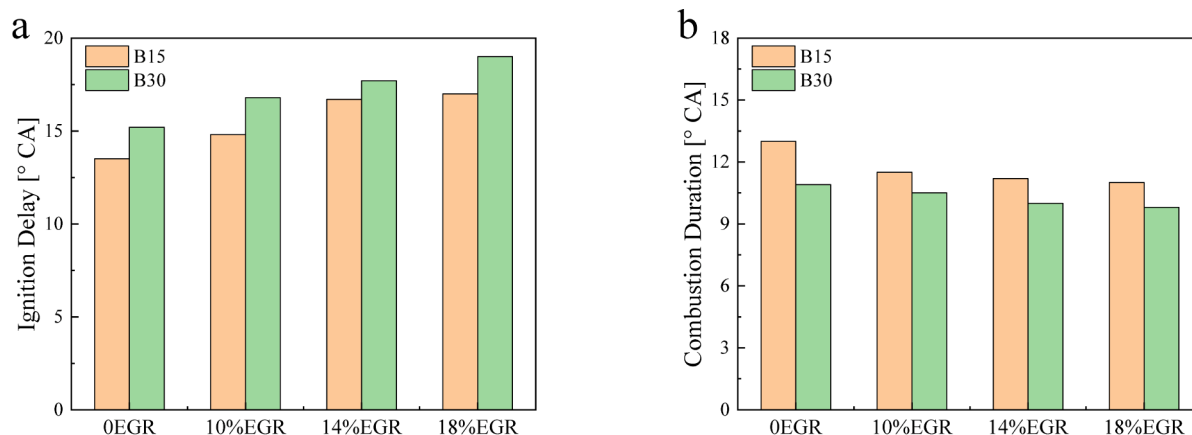


Figure 5. (a) ID of B15 and B30 at different EGR rates and (b) CD of B15 and B30 at different EGR rates.

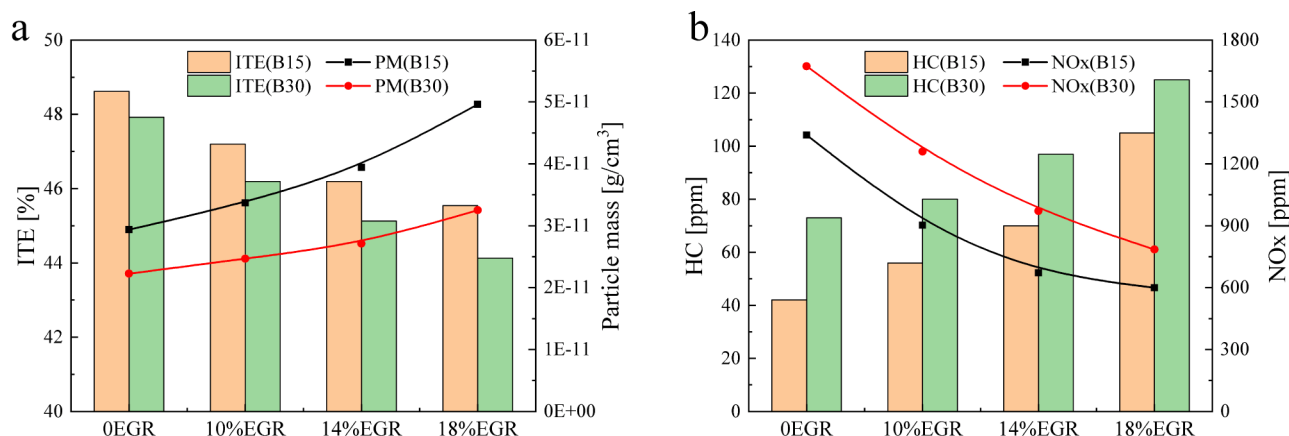


Figure 6. (a) Thermal efficiencies of B15 and B30 at different EGR rates. (b) Pollutant emissions of B15 and B30 at different EGR rates.

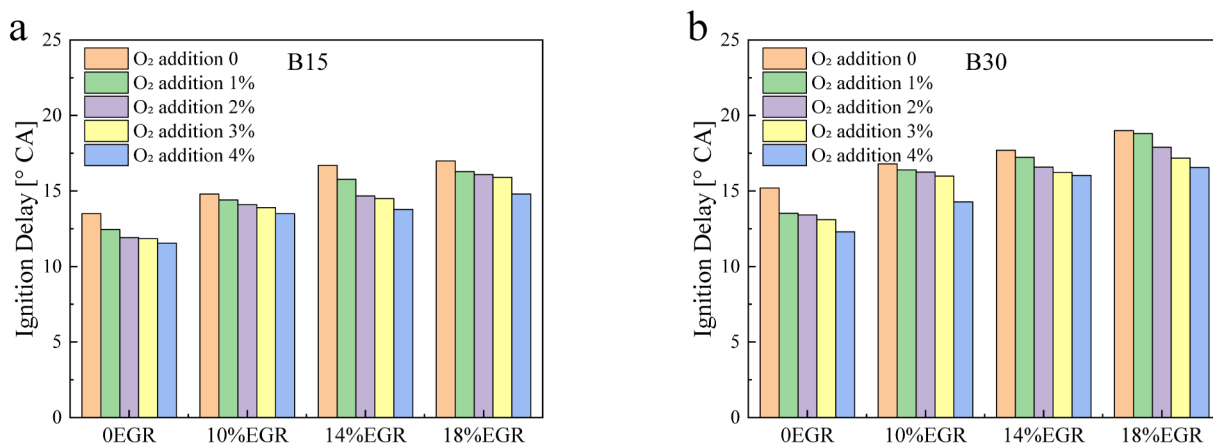


Figure 7. ID of B15 and B30 burning with different intake components: (a) B15 and (b) B30.

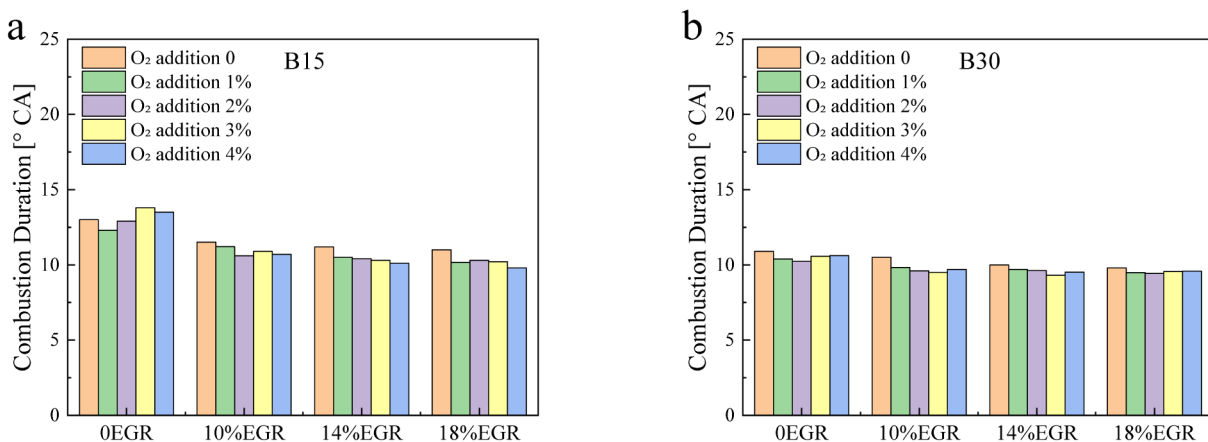


Figure 8. CD of B15 and B30 burning with different intake components: (a) B15 and (b) B30.

concentrations of B15 and B30 increase by 69% and 46%, and the HC emission of B15 and B30 increases by 150% and 71%, respectively, compared with the non-EGR condition. Among them, the increase in HC and particulate emissions verify that the low oxygen concentration caused by EGR can indeed reduce the completeness of combustion.

From the analysis above, it can be concluded that when burning the *n*-butanol/diesel blends, EGR is an effective technique to reduce the NO_x, but it also leads to combustion deterioration and thermal efficiency reduction.

2.3. Effects of EGR and Intake Oxygen Addition on Combustion and Emissions of *n*-Butanol/Diesel Blends.

To alleviate the negative effects of EGR in the case of burning the *n*-butanol/diesel blends, the effects of oxygen introduction together with the EGR gas on combustion and emissions characteristics of the engine were experimentally studied.

Figures 7 and 8 illustrate the ID and CD of B15 and B30 with different intake components. Under the same EGR rate conditions, different oxygen addition rates were tested. It is found that the ID is shortened with the increased oxygen

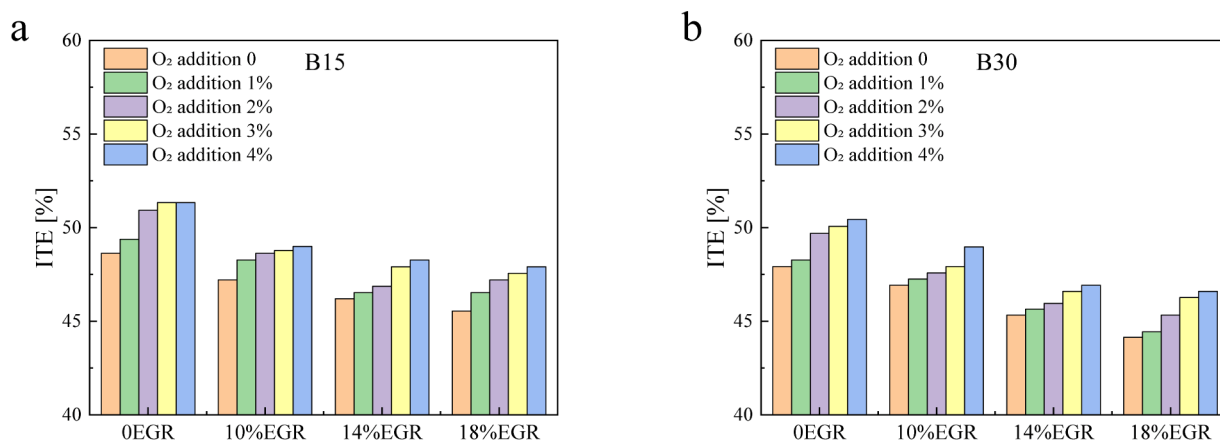


Figure 9. ITE of B15 and B30 burning with different intake components: (a) B15 and (b) B30.

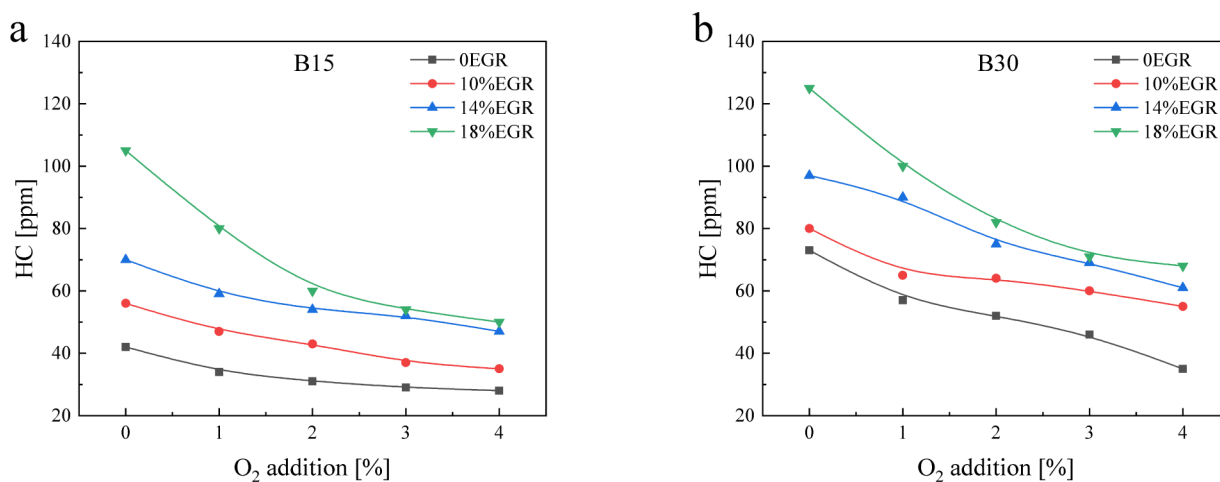


Figure 10. HC emissions of B15 and B30 burning with different intake components: (a) B15 and (b) B30.

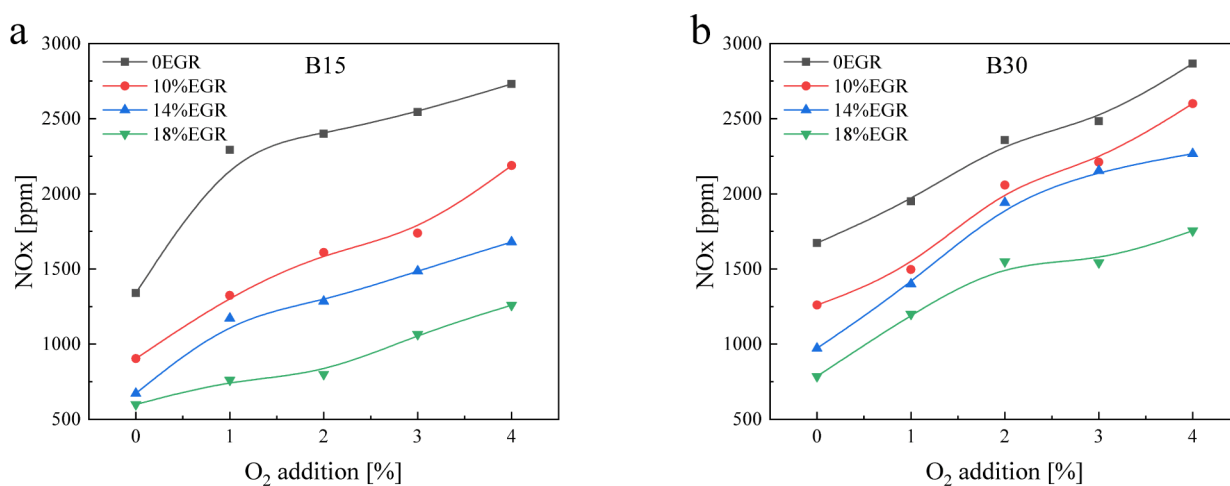


Figure 11. NO_x emissions of different fuels with different intake components: (a) B15 and (b) B30.

addition for all conditions. Comparing the effects of different oxygen addition rates under different EGR rates, it can be observed that the ID is more sensitive to the change in oxygen addition at all EGR levels and fuels. This can be explained by the fact that in-cylinder oxygen concentration is an important condition for CI, and higher in-cylinder oxygen concentration facilitates autoignition of the oil–gas mixture. However, although increasing the in-cylinder oxygen concentration

shortens the ID and reduces the premixed combustion fraction and higher in-cylinder oxygen concentration can promote the combustion process, the combined effects of the two reasons cause slight changes in the CD with the increased oxygen addition.

Since the oxygen addition rate affects ID and CD, the engine thermal efficiency can also be changed accordingly. Figure 9 shows the ITE of the engine with different intake components.

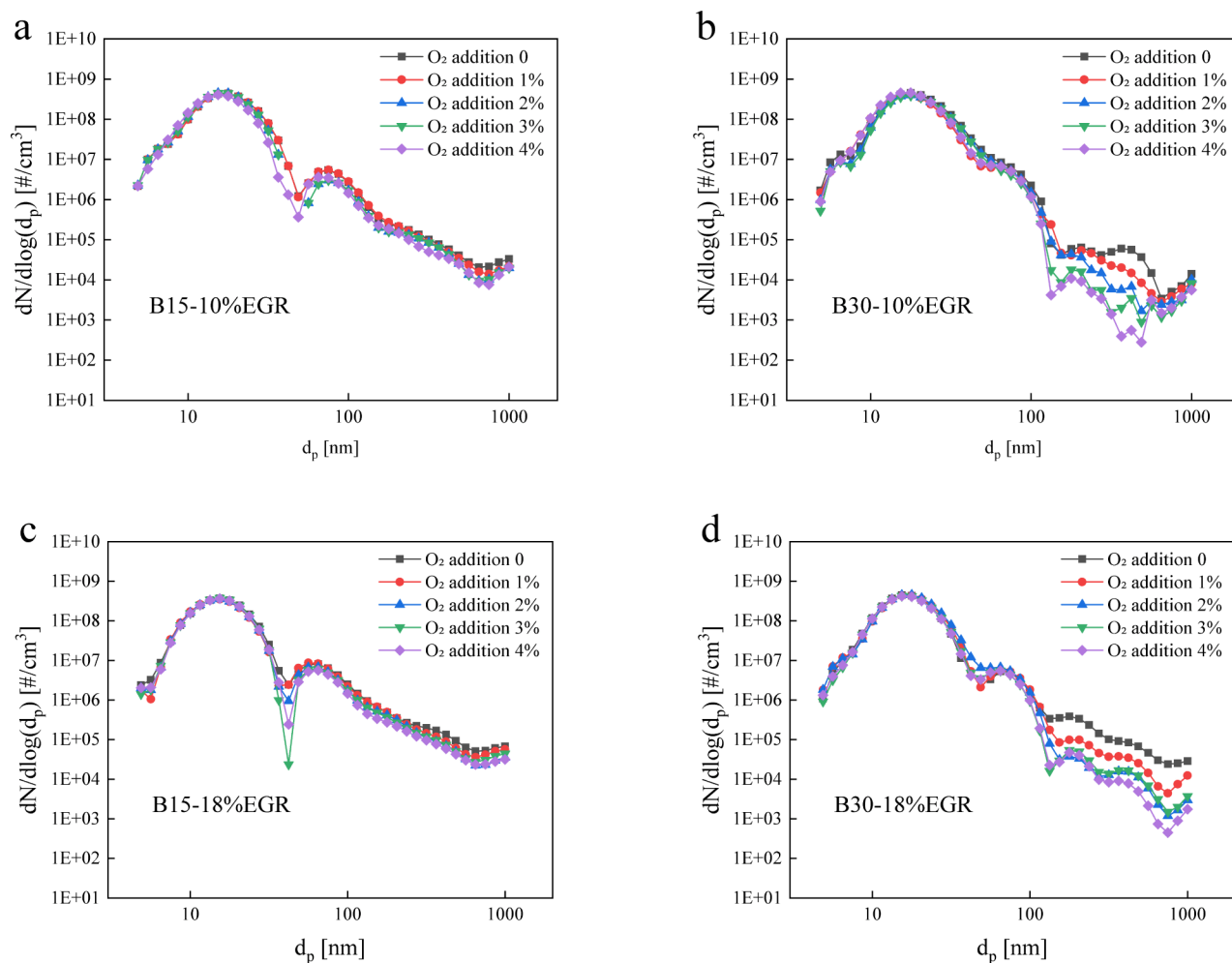


Figure 12. PSD of B15 and B30 with different intake components: (a) B15-10% EGR, (b) B30-10% EGR, (c) B15-18% EGR, and (d) B30-18% EGR.

As can be seen from the figures, oxygen addition is beneficial to improving the combustion process and compensating for the thermal efficiency reduction caused by the large proportion EGR and burning the *n*-butanol/diesel blends. Taking the 18% EGR as an example, the ITE of B15 and B30 increases by 2.4% and 2.5%, respectively, when 4% oxygen addition is introduced. This can be explained by the fact that the addition of oxygen can shorten the ID and reduce the premixed combustion fraction while maintaining a short CD. Since the in-cylinder combustion temperature is positively correlated with the premixed combustion fraction, the addition of oxygen can reduce the combustion temperature, thus reducing the heat transfer loss on the basis of maintaining the volumetricity of combustion. Additionally, the addition of oxygen is also conducive to improving incomplete combustion caused by the large proportion EGR and burning the *n*-butanol/diesel blends.

The addition of oxygen not only improves the thermal efficiency of the *n*-butanol/diesel blend fueled engine but also has a significant impact on the pollutant emissions. Figures 10 and 11 show the HC and NO_x emissions of B15 and B30 with different intake components. As can be seen from Figure 10, the oxygen addition into the intake can effectively reduce the high HC emissions caused by excessive EGR and *n*-butanol blending. Under the condition of 18% EGR rate, increasing oxygen addition to 4% can reduce HC emissions by more than

50%. This can be explained by the fact that the significant increase in the oxygen content in the cylinder is conducive to promoting HC oxidation, also increasing the in-cylinder reaction rate and temperature at the same time. As for the NO_x emissions, it can be seen from Figure 11 that the NO_x emissions increase with an increase in the oxygen addition. Under all conditions, when 4% oxygen addition is introduced into the intake, the NO_x emission is 71–150% higher than that with nonoxygen supplementation. According to Zeldovich's principle, the formation of NO_x is greatly affected by oxygen concentration, in-cylinder temperature, and its duration. The oxygen supplementation provides favorable conditions for the NO_x formation, thus promoting the chemical reaction to move toward the direction of NO_x formation.³³ Generally speaking, although increasing the oxygen content in the blended fuel and intake gas leads to the NO_x emission deterioration, the deterioration level is not very high when the EGR is applied, due to the alleviating effect of EGR on the NO_x emission.

2.4. Effects of EGR and Intake Oxygen Addition on Particulate Characteristics of *n*-Butanol/Diesel Blends.

Since particulate emission control has always been a difficult task for CI engines, and the harm of particles of different sizes to the human body are also different, it is meaningful to analyze the particle size distribution (PSD) in detail. To further investigate the effects of EGR and oxygen addition on

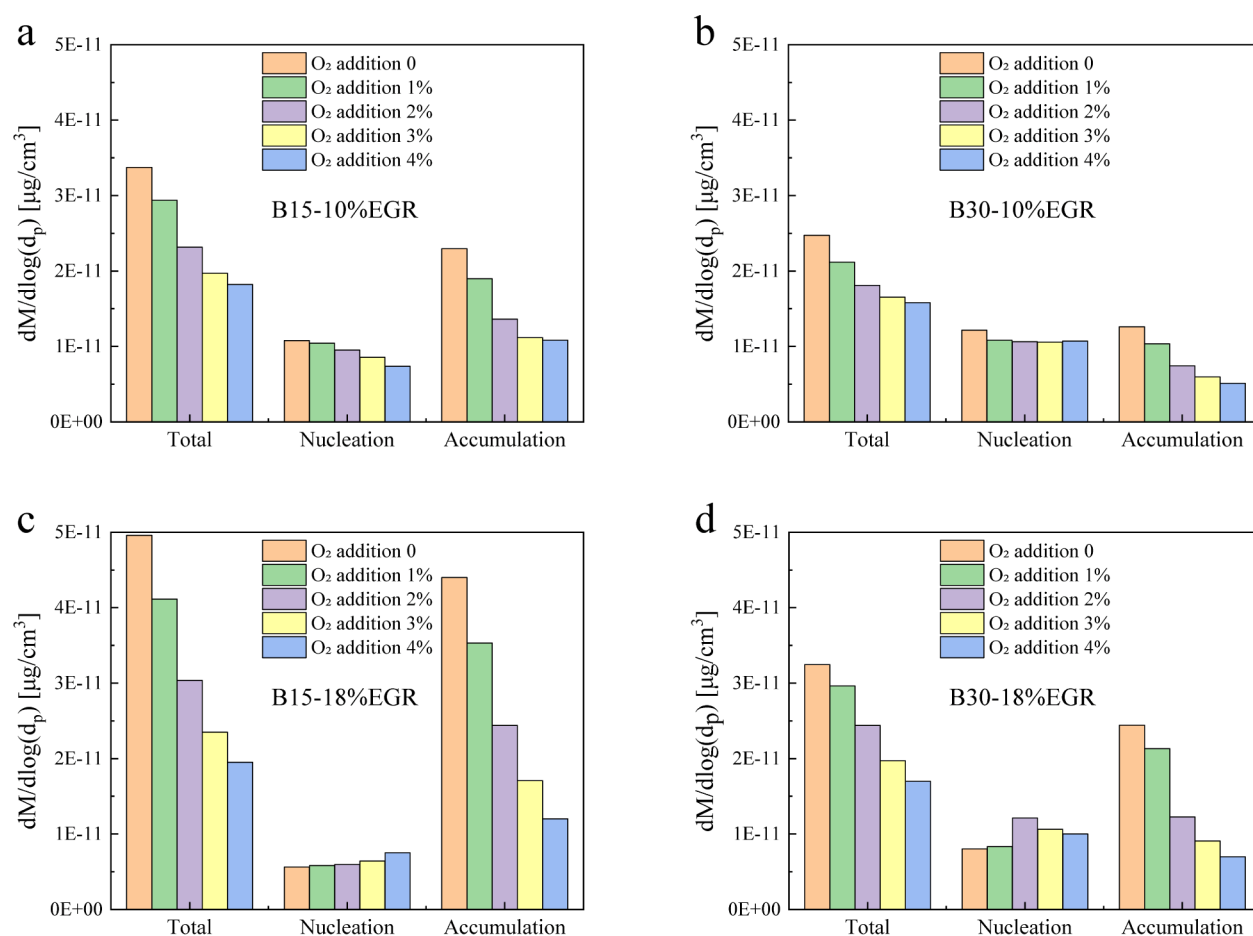


Figure 13. Mass concentration of the particles obtained with different intake components: (a) B15-10% EGR, (b) B30-10% EGR, (c) B15-18% EGR, and (d) B30-18% EGR.

particulate emission of the *n*-butanol/diesel blends, the particulate emission characteristics at different intake components were studied under the EGR rates of 10% and 18%.

Figure 12 shows the PSD of B15 and B30 with different intake components. As can be seen from Figure 12, the PSD presents a two-peak shape under all conditions, and the two peaks represent the different modes of particles, within the range of 5–35 nm (NMP) and 35–1000 nm (AMP), respectively. Moreover, the peak of NMP is an order of magnitude higher than the peak of AMP under all conditions, which indicates that the number concentration of NMP is accounted for the majority of particle number emissions when the blended fuels are used. It can also be seen that the NMP distributions almost remain constant with a change in the oxygen concentration, but the AMP decreases with an increase in the oxygen concentration, which means that the addition of oxygen can effectively promote the late oxidation of AMP. In addition, the number of the particles larger than 150 nm when burning B30 is significantly lower than that when burning B15 at the same EGR rates and oxygen addition. This indicates that the addition of *n*-butanol is particularly effective in reducing the particles with a large size.

To quantify the particle emissions in different modes, the mass concentration of NMP, AMP, and total particles calculated from the PSD are shown in Figure 13. It can be found that with an increase in EGR, the mass of NMP gradually decreases and the mass of AMP gradually increases for B15 and B30. As can be seen from Figure 13, increasing the

oxygen concentration can effectively reduce the total PM at all EGR rates and fuels. Moreover, the effects of oxygen concentration on total PM are more obvious under the conditions of the high EGR rate and low *n*-butanol-blended ratio whose total particle mass emission is relatively high. For the B30 fuels, when the addition oxygen concentration increased from 0% to 4%, the total particle mass at 10% EGR and 18% EGR decreased by 36.1% and 47.7%, respectively. For the 18% EGR rate, when the addition oxygen concentration increased from 0% to 4%, the total particle mass at B15 and B30 is reduced by 60.6% and 47.7%, respectively. In addition, the mass of AMP decreases continuously with an increase in the oxygen concentration, but the change in NMP mass with the oxygen concentration shows different trends at different EGR rates and fuels. This is because AMP is mainly formed in the local hypoxic zone due to the uneven distribution of oxygen concentration during the diffusion combustion process.^{34,35} Introducing oxygen into the intake is conducive to improving the in-cylinder oxygen concentration distribution, reducing the local hypoxic zone, thereby suppressing the formation of AMP. For NMP, although increasing the in-cylinder oxygen concentration is beneficial to reducing the unburned HC and thus suppressing the generation of nuclear particles, but at the same time, oxygen addition reduces the mass concentration of AMP, so it stunts the adsorption of gaseous precursors such as sulfuric acid and HC on the surface of AMP, thus increasing the NMP emission. The synergistic effects of these two reasons cause NMP to

show different trends with the increased oxygen concentration under different conditions.

In summary, oxygen addition can effectively improve the ITE and suppress HC and particle emission, but the NO_x emission can be increased. Compared with using EGR only, the combination of EGR and oxygen addition can improve the thermal efficiency and maintain relatively low pollutant emissions when burning the *n*-butanol/diesel blends.

2.5. Comparative Analysis for This Study. To intuitively evaluate the effects of blending *n*-butanol, EGR, and oxygen addition on the combustion and emissions performance of the engine, the thermal efficiency and main emissions of the engine are listed in Table 1 when the abovementioned technologies are used.

Table 1. Comparison of the ITE and Emission Result Obtained Using Different Technologies

fuel	EGR rate (%)	O ₂ addition (%)	ITE (%)	NO _x (ppm)	PM (μg/cm ³)	HC (ppm)
diesel	0	0	49.5	1150	8.71×10^{-11}	25
B15	0	0	48.6	1340	2.94×10^{-11}	42
B30	18	0	44.1	785	3.25×10^{-11}	125
B15	18	2	47.2	800	3.04×10^{-11}	60

As can be seen from Table 1, burning the *n*-butanol/diesel blends can significantly reduce particulate emissions, but it causes an increase in NO_x and HC and a decrease in ITE. For the combination of *n*-butanol blends and EGR, the use of a large proportion of *n*-butanol and a high EGR rate can simultaneously reduce NO_x and PM compared to the original condition, but the ITE and HC emissions further deteriorate under that condition. Moreover, compared with the combination of *n*-butanol/diesel blends and EGR, further adding oxygen into the intake can achieve excellent engine performance. By adjusting the *n*-butanol ratio, EGR rate, and oxygen concentration, the ITE can be restored and lower PM and HC emissions are achieved on the basis of a slight change in NO_x emission.

3. CONCLUSIONS

Combining different intake components, the combustion and emissions characteristics of CI engine fueled with *n*-butanol/diesel blends were studied and analyzed in this paper. The results show that when burning the *n*-butanol/diesel blends, the synergistic effect of EGR and oxygen addition can effectively reduce the emissions of NO_x and particle, while keeping the thermal efficiency basically unchanged. The conclusions were drawn as follows:

(1) At medium speed and load, with the increased *n*-butanol volume fraction of the *n*-butanol/diesel blends, the ID prolongation and CD shortening lead to a significant decrease in particulate emission. However, the NO_x and HC emissions of B15 and B30 are higher than that of diesel.

(2) With the increased EGR rate, the *n*-butanol/diesel blend fueled engine can effectively suppress NO_x emissions, but it causes the deterioration of HC and particulate emissions. Naturally, ITE decreases accordingly.

(3) With an increase in oxygen addition, the ID is shortened but the CD is not changed significantly. Compared with the combination of *n*-butanol/diesel blends and EGR, by further adding oxygen into the intake, the ITE can be restored with

lower PM and HC emissions being achieved on the basis of a slight change in NO_x emission.

(4) With an increase in the EGR rate, the AMP and total PM emission of B15 and B30 increase significantly, but the mass concentration of NMP is decreased. Benefiting from the high oxygen concentration can effectively reduce the number and mass concentration of AMP particles, and the addition of oxygen can significantly suppress the total exhaust particle mass concentration, especially for the conditions of high EGR rates and low *n*-butanol-blended ratios.

4. EXPERIMENTAL SYSTEM AND TEST PROCEDURE

4.1. Experimental Engine and Apparatus. The experimental engine was a single-cylinder engine modified from a four-cylinder, four-valve, common-rail diesel engine. The main engine specifications are shown in Table 2. The third

Table 2. Engine Specifications

category	properties
geometric compression ratio	17.7
cylinder diameter (mm)	95.4
piston stroke (mm)	104.9
connecting rod length (mm)	162
intake valve closing moment (deg CA ATDC)	-143
exhaust valve closing moment (deg CA ATDC)	366
injector orifice number	6
injector orifice diameter (mm)	0.12
oil jet cone angle (°)	12
Eddy current ratio	0.97

cylinder of the engine was kept as the working cylinder with independent intake/exhaust system and fuel supply system; the valve and fuel injector of the other cylinders are removed and the others remain unchanged. An opened ECU (NI2106), which can modify the fuel injection parameters flexibly, was used in the engine. Figure 14 shows the schematic diagram of the experimental setup. To adjust the intake components and intake pressure flexibly, a two-stage supercharging system and an intake component control system were designed and fixed to the engine. In this study, pure CO₂ was used to simulate the EGR gas. A compressor together with a pressure sensor and a current limiting valve were employed to adjust the intake air pressure within a range of 0.1–0.3 MPa. Intake component control equipment was developed based on a FXSU-32M programmable logic controller (PLC) worked under a self-edited program. PLC was used to adjust the proportions of the pure O₂ and pure CO₂ both supplied with the high-pressure tank. The flux of O₂ and CO₂ can be adjusted flexibly by magnetic valves in the range of 0–100 L/min. Figure 15 shows the main structure of the intake oxygen system.

The main instruments and equipment of the measuring and control system are shown in Table 3. Among them, the characteristics of the particulate emission were measured using the DMS500 fast particle analyzer. When the cyclone separator is introduced in DMS500, large particles (particle diameter larger than 1000 nm) of engine exhaust are removed, and then the sample gas enters the classifier to classify the charged particles according to the electron mobility. Finally, the classified particles generate corresponding currents in the electrometer to determine the concentration of particles with different sizes.³⁶ The particle mass can be calculated based on the number of the particles using the following formula:

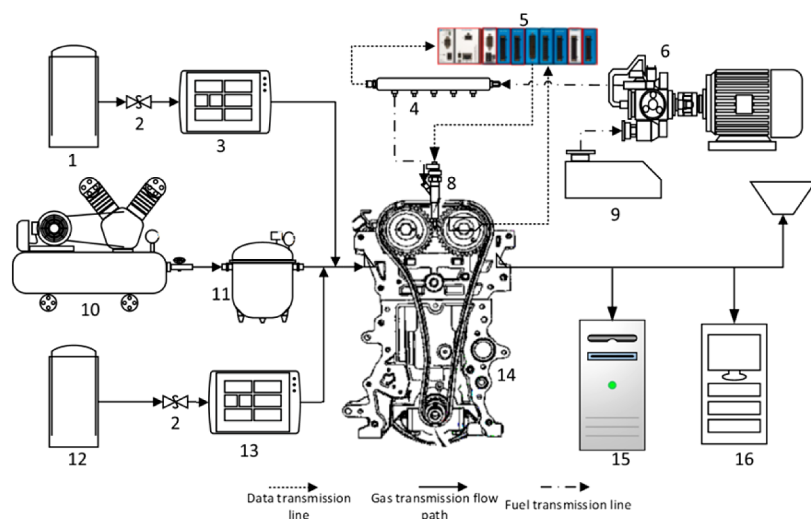


Figure 14. Schematic diagram of the experimental setup: 1: high-pressure oxygen cylinder; 2: pressure-reducing valve; 3: intake oxygen control machine; 4: high-pressure oil rail; 5: ECU; 6: high-pressure oil pump; 7: alternating current motor; 8: injector; 9: fuel tank; 10: compressor; 11: pressure-stabilizing tank; 12: CO₂ cylinder; 13: intake CO₂ control machine; 14: engine; 15: engine exhaust particle sizer; and 16: fast engine exhaust analyzer.

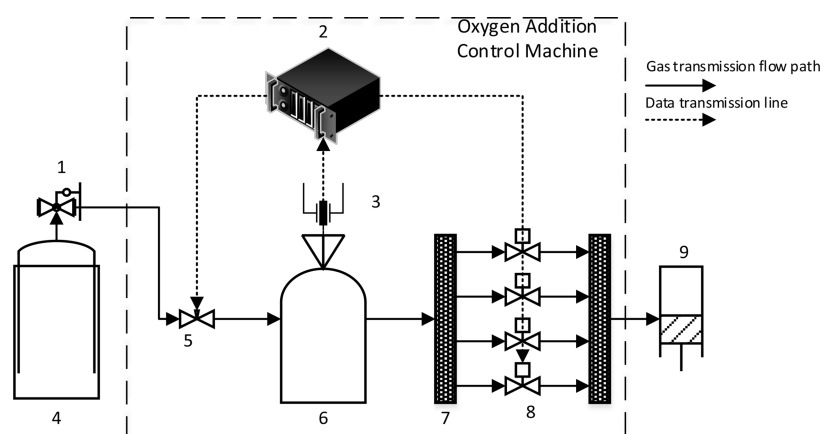


Figure 15. Schematic representation of the intake oxygen system: 1: O₂ decompression valve; 2: PLC; 3: pressure sensor; 4: high-pressure oxygen tank; 5: solenoid valve; 6: pressure regulator; 7: O₂ distributor; 8: high-frequency solenoid valve; and 9: engine.

Table 3. Main Equipment

category	measuring instruments	manufacturer	accuracy
dynamometer	CW260	CAMA	torque: ± 0.5 NM speed: ± 2 rpm
fuel flow meter	FX-100	ONO-SOKKI	$\pm 0.12\%$
air flow meter	20R100	TOCEL	$\pm 1\%$
CO and CO ₂	NDIR500	Cambustion	$< 2\%$ FS/h
HC	HFR500	Cambustion	$< 1\%$ FS/h
NO _x	CLD500	Cambustion	< 5 ppm/h
particle	DMS500	Cambustion	

$$\text{mass}_{\text{agg}} (\mu\text{g}) = 2.20 \times n_{\text{agg}} \times 10^{-15} d_p^{2.65} (\text{nm})$$

where d_p is the particle size, mass_{agg} is the mass of the particles with the size d_p , and n_{agg} is the number of particles with the size d_p .

4.2. Methodology and Test Conditions. The ultralow sulfur diesel was used as the baseline fuel. The pure baseline diesel was defined as B0. One comparative fuel was made of 85% baseline diesel and 15% *n*-butanol (by volume), defined as

B15. Another comparative fuel was composed of 70% baseline diesel and 30% *n*-butanol (by volume), defined as B30. Table 4 shows the main properties of the fuels for test. Table 5 summarizes the experimental conditions of this study. The

Table 4. Main Properties of Tested Fuels

fuel property	method	B0	B15	B30
density (kg m ⁻³)	ASTM 4052	837.5	830.5	826.5
cetane number	ASTM D613	52.3	48.34	44.33
low heating value (MJ kg ⁻¹)	ASTM D4809	43.88	41.65	40.15
total aromatics (%)	ASTM D1319	≤ 11	≤ 9.4	≤ 7.79
latent heat of vaporization (kJ kg ⁻¹)		270	315.71	361.94
elements				
S (10 ⁻⁶)	ASTM D5453	≤ 10	≤ 8.55	≤ 7.08
C (%)	ASTM D5291	86.12	83.04	79.91
H (%)		13.84	13.79	13.75
O (%)		0	3.14	6.31

Table 5. Engine Operating Conditions

category	properties
engine speed	1400 rpm
average indicative pressure	~0.85 MPa
injection pressure	100 MPa
CA50	~8 deg CA ATDC
inlet air temperature	25 ± 1 °C
cooling water temperature	80 ± 1 °C

engine runs with a maximum torque speed of 1400 rpm, under a load rate of 50%. The indicated mean effective pressure (IMEP) was about 0.85 MPa. For different fuels and intake components, the fuel injection timing was adjusted to ensure that the heat release center (CA50) was 8 deg CA ATDC, and the injection pressure was kept at 100 MPa. The different intake components were achieved by changing the oxygen addition and EGR rate. Without the oxygen addition, the EGR rate determines the oxygen concentration in the intake gas, and the existing research results show that the excessive oxygen introduction leads to a significant deterioration of the NO_x emissions.³⁷ Therefore, depending on the actual situation, this experiment supplies oxygen in moderation (1–4% with the step of 1%) for all of the EGR rate conditions including 0%, 10%, 14%, and 18%, respectively. All the tests were repeated three times, and the data used in this paper are the average of the three tests. Among them, the EGR rate was defined as the mass ratio of the CO₂ content in the intake to the exhaust of the engine, and 1–4% oxygen addition refers to the introduction of oxygen with a mass fraction addition of 1–4% on the basis of the intake oxygen concentration when EGR is introduced. The difference between the combustion start point (CA10) and the fuel injection start point is defined as ID, and the difference between the combustion end point (CA90) and the CA10 is defined as CD.

AUTHOR INFORMATION

Corresponding Author

Hao Zhang – State Key Laboratory of Automotive Simulation and Control, Jilin University, Changchun 130025, China;
 orcid.org/0000-0002-7499-5114; Email: 771388497@qq.com

Authors

Wanchen Sun – State Key Laboratory of Automotive Simulation and Control, Jilin University, Changchun 130025, China

Xin Zhang – State Key Laboratory of Automotive Simulation and Control, Jilin University, Changchun 130025, China

Liang Guo – State Key Laboratory of Automotive Simulation and Control, Jilin University, Changchun 130025, China

Yi Sun – State Key Laboratory of Automotive Simulation and Control, Jilin University, Changchun 130025, China

Yuying Yan – Faculty of Engineering, University of Nottingham, Nottingham NG7 2RD, U.K.

Jun Li – State Key Laboratory of Automotive Safety and Energy, Tsinghua University, Beijing 100084, China

Dongqi Fu – State Key Laboratory of Automotive Simulation and Control, Jilin University, Changchun 130025, China

Complete contact information is available at:

<https://pubs.acs.org/10.1021/acsoomega.1c02014>

Notes

The authors declare no competing financial interest.

ACKNOWLEDGMENTS

This work was supported by the National Natural Science Foundation of China (Project code nos. 51476069 and 51676084); the Jilin Provincial Industrial Innovation Special Guidance Fund Project (Project code no. 2019C058-3); the Jilin Province Science and Technology Development Plan Project (Project code no. 20180101059JC); and the Jilin Province Specific Project of Industrial Technology Research & Development (Project code no. 2020C025-2).

REFERENCES

- (1) Wang, X. G.; Zheng, B.; Huang, Z. H.; Zhang, N.; Zhang, Y. J.; Hu, E. J. Performance and Emissions of a Turbocharged, High-Pressure Common Rail Diesel Engine Operating on Biodiesel/Diesel Blends. *Proc. Inst. Mech. Eng., Part D* **2010**, *225*, 127–139.
- (2) Topinka, J.; Rossner, P.; Stolcpartova, J.; Schmuczerova, J.; Milcova, A.; Hruha, E.; Machala, M. Comparison of genotoxic effects of major diesel exhaust components in human alveolar basal epithelial cells (A549). *Toxicol. Lett.* **2014**, *229*, No. S155.
- (3) Ma, X.; Zhang, J.; Xu, H.; Shuai, S.; Price, P. Particulate matter characteristics of a light-duty diesel engine with alternative fuel blends. *Proc. Inst. Mech. Eng., Part D* **2014**, *228*, 1516–1529.
- (4) Shen, Z.; Cui, W.; Liu, Z.; Tian, J.; Wu, S.; Yang, J. Distribution evolution of intake and residual gas species during CO₂ stratification combustion in diesel engine. *Fuel* **2016**, *166*, 427–435.
- (5) Petranović, Z.; Vujanović, M.; Duić, N. Towards a more sustainable transport sector by numerically simulating fuel spray and pollutant formation in diesel engines. *J. Cleaner Prod.* **2015**, *88*, 272–279.
- (6) Yan, F.; Winijkul, E.; Jung, S.; Bond, T. C.; Streets, D. G. Global emission projections of particulate matter (PM): I. Exhaust emissions from on-road vehicles. *Atmos. Environ.* **2011**, *45*, 4830–4844.
- (7) Demirbas, A. Political, economic and environmental impacts of biofuels: A review. *Appl. Energy* **2009**, *86*, S108–S117.
- (8) Agarwal, A. K. Biofuels (alcohols and biodiesel) applications as fuels for internal combustion engines. *Prog. Energy Combust. Sci.* **2007**, *33*, 233–271.
- (9) Mahla, S. K.; Dhir, A.; Gill, K. J. S.; Cho, H. M.; Lim, H. C.; Chauhan, B. S. Influence of EGR on the simultaneous reduction of NO_x-smoke emissions trade-off under CNG-biodiesel dual fuel engine. *Energy* **2018**, *152*, 303–312.
- (10) Mohsin, R.; Majid, Z. A.; Shihnan, A. H.; Nasri, N. S.; Sharer, Z. Effect of biodiesel blends on engine performance and exhaust emission for diesel dual fuel engine. *Energy Convers. Manage.* **2014**, *88*, 821–828.
- (11) Dubey, P.; Gupta, R. Effects of dual bio-fuel (Jatropha biodiesel and turpentine oil) on a single cylinder naturally aspirated diesel engine without EGR. *Appl. Therm. Eng.* **2017**, *115*, 1137–1147.
- (12) Zhang, H.; Guo, L.; Yan, Y.; Sun, W.; Li, J.; Wang, Q.; Sun, Y. Experimental investigation on the combustion and emissions characteristics of an n-butanol/CTL dual fuel engine. *Fuel* **2020**, *274*, No. 117696.
- (13) Ujor, V.; Bharathidasan, A. K.; Cornish, K.; Ezeji, T. C. Feasibility of producing butanol from industrial starchy food wastes. *Appl. Energy* **2014**, *136*, 590–598.
- (14) Zheng, Z.; Yue, L.; Liu, H.; Zhu, Y.; Zhong, X.; Yao, M. Effect of two-stage injection on combustion and emissions under high EGR rate on a diesel engine by fueling blends of diesel/gasoline, diesel/n-butanol, diesel/gasoline/n-butanol and pure diesel. *Energy Convers. Manage.* **2015**, *90*, 1–11.
- (15) Sukjit, E.; Herreros, J. M.; Dearn, K. D.; García-Contreras, R.; Tsolakis, A. The effect of the addition of individual methyl esters on the combustion and emissions of ethanol and butanol-diesel blends. *Energy* **2012**, *42*, 364–374.

- (16) Zhang, Q.; Yao, M.; Zheng, Z.; Liu, H.; Xu, J. Experimental study of n-butanol addition on performance and emissions with diesel low temperature combustion. *Energy* **2012**, *47*, 515–521.
- (17) Kheyrandish, M.; Asadollahi, M. A.; Jeihanipour, A.; Doostmohammadi, M.; Rismani-Yazdi, H.; Karimi, K. Direct production of acetone–butanol–ethanol from waste starch by free and immobilized *Clostridium acetobutylicum*. *Fuel* **2015**, *142*, 129–133.
- (18) Li, J.; Chen, X.; Qi, B.; Luo, J.; Zhang, Y.; Su, Y.; Wan, Y. Efficient production of acetone–butanol–ethanol (ABE) from cassava by a fermentation–pervaporation coupled process. *Bioresour. Technol.* **2014**, *169*, 251–257.
- (19) Zhou, X.; Song, M.; Huang, H.; Yang, R.; Wang, M.; Sheng, J. Numerical Study of the Formation of Soot Precursors during Low-Temperature Combustion of a n-Butanol–Diesel Blend. *Energy Fuels* **2014**, *28*, 7149–7158.
- (20) Merola, S. S.; Tornatore, C.; Iannuzzi, S. E.; Marchitto, L.; Valentino, G. Combustion process investigation in a high speed diesel engine fuelled with n-butanol diesel blend by conventional methods and optical diagnostics. *Renewable Energy* **2014**, *64*, 225–237.
- (21) Zheng, Z.; Li, C.; Liu, H.; Zhang, Y.; Zhong, X.; Yao, M. Experimental study on diesel conventional and low temperature combustion by fueling four isomers of butanol. *Fuel* **2015**, *141*, 109–119.
- (22) Rakopoulos, D. C.; Rakopoulos, C. D.; Giakoumis, E. G.; Dimaratos, A. M.; Kyritsis, D. C. Effects of butanol–diesel fuel blends on the performance and emissions of a high-speed DI diesel engine. *Energy Convers. Manage.* **2010**, *51*, 1989–1997.
- (23) Gu, X.; Li, G.; Jiang, X.; Huang, Z.; Lee, C.-F. Experimental study on the performance of and emissions from a low-speed light-duty diesel engine fueled with n-butanol–diesel and isobutanol–diesel blends. *Proc. Inst. Mech. Eng., Part D* **2012**, *227*, 261–271.
- (24) Yao, M.; Wang, H.; Zheng, Z.; Yue, Y. Experimental study of n-butanol additive and multi-injection on HD diesel engine performance and emissions. *Fuel* **2010**, *89*, 2191–2201.
- (25) Cheng, X.; Li, S.; Yang, J.; Liu, B. Investigation into partially premixed combustion fueled with n-butanol–diesel blends. *Renewable Energy* **2016**, *86*, 723–732.
- (26) Şahin, Z.; Aksu, O. N. Experimental investigation of the effects of using low ratio n-butanol/diesel fuel blends on engine performance and exhaust emissions in a turbocharged DI diesel engine. *Renewable Energy* **2015**, *77*, 279–290.
- (27) Huang, Y.; Li, Y.; Luo, K.; Wang, J. Biodiesel/butanol blends as a pure biofuel excluding fossil fuels: Effects on diesel engine combustion, performance, and emission characteristics. *Proc. Inst. Mech. Eng., Part D* **2020**, *234*, 2988–3000.
- (28) Dinesha, P.; Nayak, V.; Mohanan, P. Effect of oxygen enrichment on the performance, combustion, and emission of single cylinder stationary CI engine fueled with cardanol diesel blends. *J. Mech. Sci. Technol.* **2014**, *28*, 2919–2924.
- (29) Li, Q.; Zhao, C.; Chen, X.; Wu, W.; Li, Y. Comparison of pulverized coal combustion in air and in O₂/CO₂ mixtures by thermogravimetric analysis. *J. Anal. Appl. Pyrolysis* **2009**, *85*, 521–528.
- (30) Liang, Y.; Shu, G.; Wei, H.; Zhang, W. Effect of oxygen enriched combustion and water–diesel emulsion on the performance and emissions of turbocharged diesel engine. *Energy Convers. Manage.* **2013**, *73*, 69–77.
- (31) Song, J.; Zello, V.; Boehman, A. L.; Waller, F. J. Comparison of the Impact of Intake Oxygen Enrichment and Fuel Oxygenation on Diesel Combustion and Emissions. *Energy Fuels* **2004**, *18*, 1282–1290.
- (32) Byun, H.; Hong, B.; Lee, B. The effect of oxygen enriched air obtained by gas separation membranes from the emission gas of diesel engines. *Desalination* **2006**, *193*, 73–81.
- (33) Ladommatos, N.; Abdelhalim, S. M.; Zhao, H.; Hu, Z.; Dilution, T. Chemical, and Thermal Effects of Exhaust Gas Recirculation on Diesel Engine Emissions—Part 1: Effect of Reducing Inlet Charge Oxygen. *SAE International*, **1996**.
- (34) Desantes, J.; Bermudez, V.; Garcia, A.; Linares, W.; Kolodziej, C. An Investigation of Particle Size Distributions with Post Injection in DI Diesel Engines; *SAE International*, 2011.
- (35) Wang, Q.; Sun, W.; Guo, L.; Fan, L.; Cheng, P.; Li, G.; Du, J. Particle number size distribution from direct-injection premixed combustion engine fueled with gasoline/diesel blends. *Proc. Inst. Mech. Eng., Part D* **2019**, *234*, 258–269.
- (36) Chuepeng, S.; Xu, H.; Tsolakis, A.; Wyszynski, M.; Price, P. Particulate matter size distribution in the exhaust gas of a modern diesel engine fuelled with a biodiesel blend. *Biomass Bioenergy* **2011**, *35*, 4280–4289.
- (37) Assanis, D. N.; Poola, R. B.; Sekar, R.; Cataldi, G. R. Study of using oxygen-enriched combustion air for locomotive diesel engines. *J. Eng. Gas Turbines Power* **2001**, *123*, 157–166.